EPS 28th Conference on Controlled Fusion and Plasma Physics, Funchal, Portugal (18.-22.6.2001)

Influence of flux surface shape on microinstabilities and turbulence

A. Kendl and B. Scott

Max-Planck-Institut für Plasmaphysik, EURATOM Association,
D-85748 Garching bei München, Germany

Tokamak and stellarator flux surface shape enters into both drive and damping mechanisms of microinstabilities and turbulence. The assumption of circular tori ($s-\alpha$ model geometry) is known to be an oversimplification even for tokamaks, whereas strong helical variations and shaping in stellarators require use of detailed equilibria representations for drift stability calculations from the outset. We study the effects of three-dimensional general magnetic field geometry with linear gyrokinetic ITG / ETG and nonlinear drift-Alfvén fluid edge turbulence simulations.

I. LINEAR GYROKINETIC ITG/ETG THEORY

Growth rates γ for ion-temperature-gradient (ITG) driven drift modes are obtained as solutions of the electromagnetic gyrokinetic Vlasov-Maxwell equations (GKE) in a ballooning mode representation for general 3D geometry. The linear evolution of the nonadiabatic part of the ion distribution function is simulated using an explicit initial value code [1]. The contribution of dissipative trapped electrons (DTE) is calculated perturbatively on the ion time scale. In Fig. 1, we compare measured $\Omega_{E\times B}$ shearing rates [2] with our computed ITG growth rates for an internal transport barrier (ITB) discharge and an H-mode discharge with improved confinement of the ASDEX Upgrade (AUG) experiment. The AUG equilibrium magnetic field configuration in Boozer coordinates is precalculated by the HAGIS code, using a numerical equilibrium generated from the HELENA code. Uncertainties in the simulation results (estimated 20 %) arise mainly through experimental error bars in the measured profiles. For the two investigated experimental shots (AUG #13037 and #13149) the modes are predominantly electrostatic and show only small corrections due to DTE. In the ITB case (#13149, Fig. 1 right), $\Omega_{E\times B}$ is mostly larger than or comparable to γ.

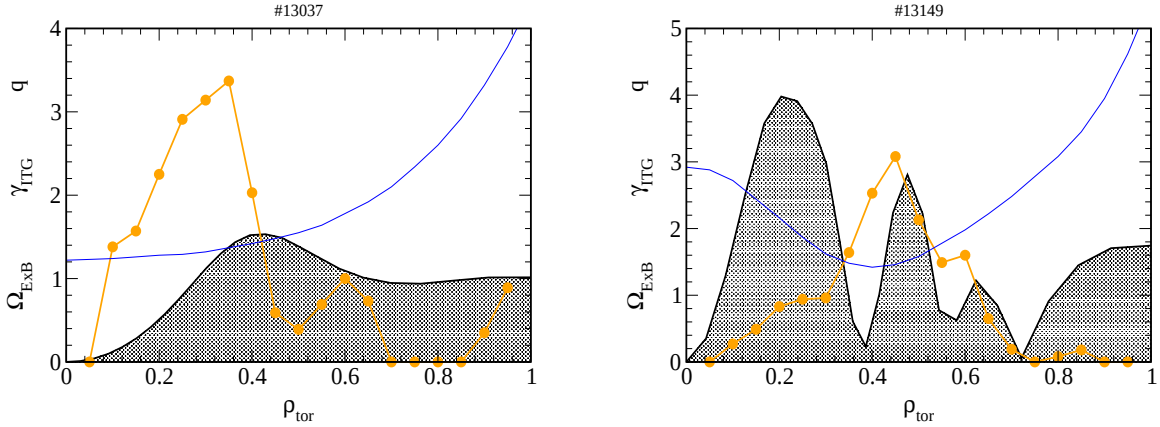

FIG. 1. Comparison of measured shearing rates [2] with ITG growth rates in ASDEX Upgrade geometry.

The differences between the two cases in Fig. 1 arise mainly through plasma and safety factor profiles, whereas the equilibrium magnetic field configuration does not change significantly. Next, we investigate the effect of Shafranov shift through rising plasma pressure in the 3D configuration of a stellarator reactor. In the Helias reactor HSR finite β leads to an increase of the magnetic well from $V'' = -0.68\%$ in the vacuum case to $V'' = -9.14\%$ for $\langle\beta\rangle = 5\%$ [3]. This enters into the GKE via the curvature drift Ω_D, where normal and geodesic curvature and local shear are modified. In Fig. 2 (left), $\Omega_D(\zeta)$ along a field line is shown for the vacuum and high β cases. The destabilizing region $\Omega_D < 0$ in ballooning space is significantly shrunk for large plasma pressure. In the k-spectra (Fig. 2 right) this is expressed in a damping of γ, and a shift of the maximum to larger $\rho_s k_\theta$ is observed due to higher elongation in the large β case.

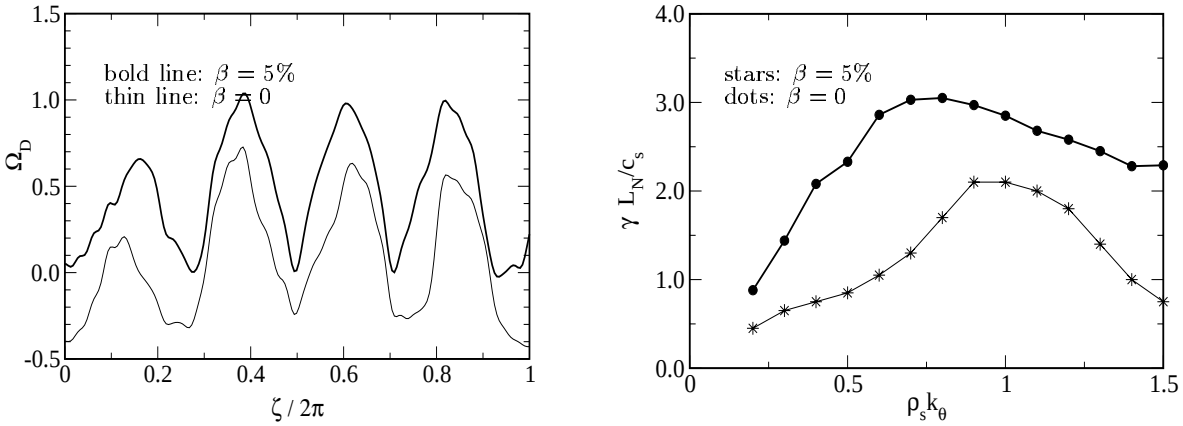

FIG. 2. Electromagnetic gyrokinetic simulations in the 3D Helias advanced stellarator reactor geometry HSR.

In recent electron-temperature-gradient (ETG) driven turbulence simulations it was found that, unlike in the corresponding ITG case, the electron heat flux is significantly underestimated by simple mixing length estimates in a certain parameter regime (shear $\hat{s} \sim 1$, low shift α) [4]. This observation is directly linked to the presence of radially highly elongated vortices ("streamers") which lead to very effective cross-field transport. Fig. 3 shows, that a linear gyrokinetic analysis of the growth rate $\gamma(k_r)$ in the $\hat{s} - \alpha$ plane is already a reliable indicator of streamer formation and shows the same features as the corresponding diagram obtained by nonlinear simulations in Ref. [4].

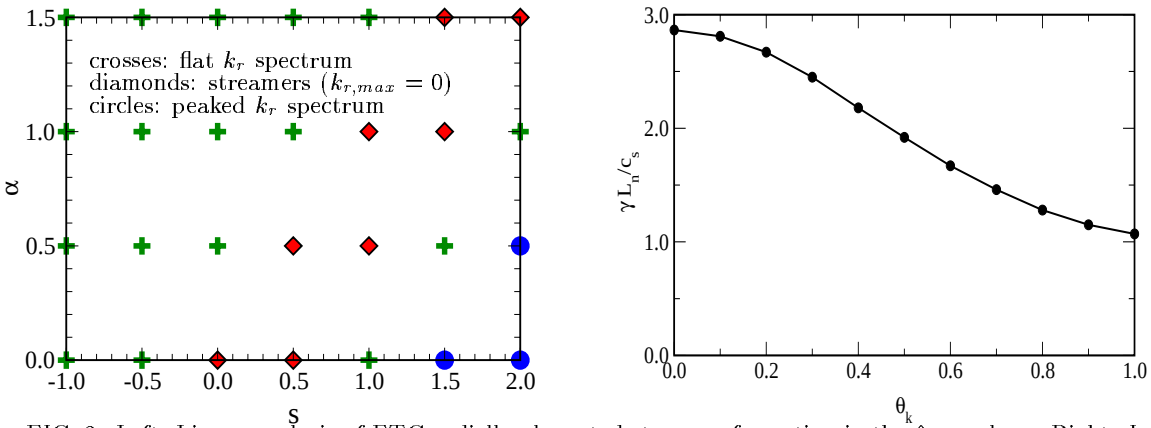

FIG. 3. Left: Linear analysis of ETG radially elongated streamer formation in the $\hat{s} - \alpha$ plane. Right: In the streamer formation region (red diamonds in the left figure) the maximum growth rate occurs for $k_r = 0$.

II. DRIFT-ALFVÉN WAVE EDGE TURBULENCE

By means of the drift-Alfven flux-tube turbulence code DALF3 [5] we have previously shown that local shear can act as an effective agent for damping of fluctuations in low-global-shear stellarators [6]. Here we systematically investigate this effect further by introducing the model geometry of a "locally sheared slab": Helical variations of local shear in N field periods, as well as strong singly peaked local shear that represents divertor X-point effects, are modelled. The latter affects the otherwise constant parallel mode structure significantly in the region of the X-point, where the turbulence level is reduced by a third. With a growing number of sinusoidal local shear periods the transport Γ_N saturates to an almost constant level for $N \geq 3$. The decreasing width of the local shear perturbations removes their effect for $N \geq 8$, and convective cell modes like in an unsheared slab develop. (Parameters were $qR/L_\perp$=135, $\hat{\nu}$=4, $\hat{\beta}$=1, μ=5, see Ref. [6])

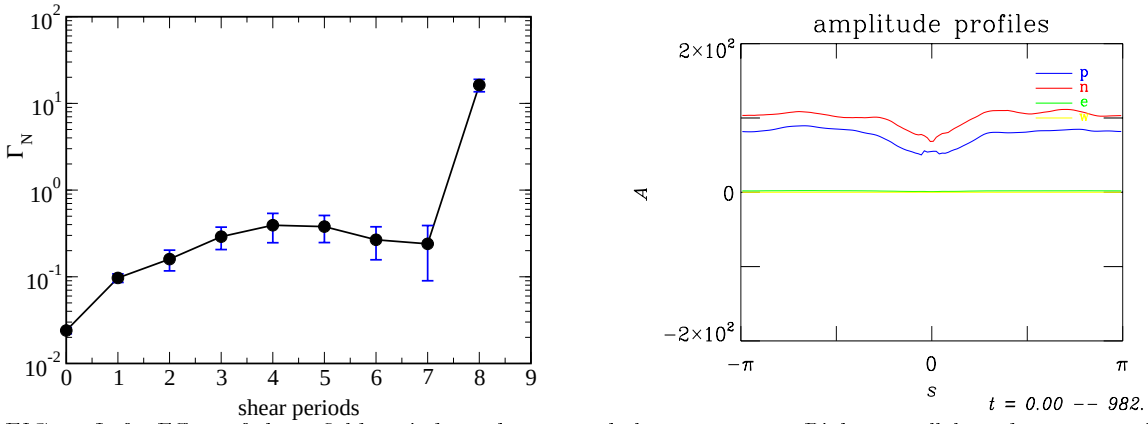

FIG. 4. Left: Effect of shear field period number on turbulent transport. Right: parallel mode structure for a modelled X-point local shear peaked at the parallel coordinate $s = 0$ in slab geometry.

As benchmark for the local shear model we have performed a series of runs varying $\hat{s}$ in a globally sheared slab without curvature. In the nonlinear saturation phase, but before the onset of zonal flows, turbulent transport Γ_N is damped with rising shear $\hat{s}$. With the full dynamics including zonal flows, the turbulence is reduced to an almost constant low level.

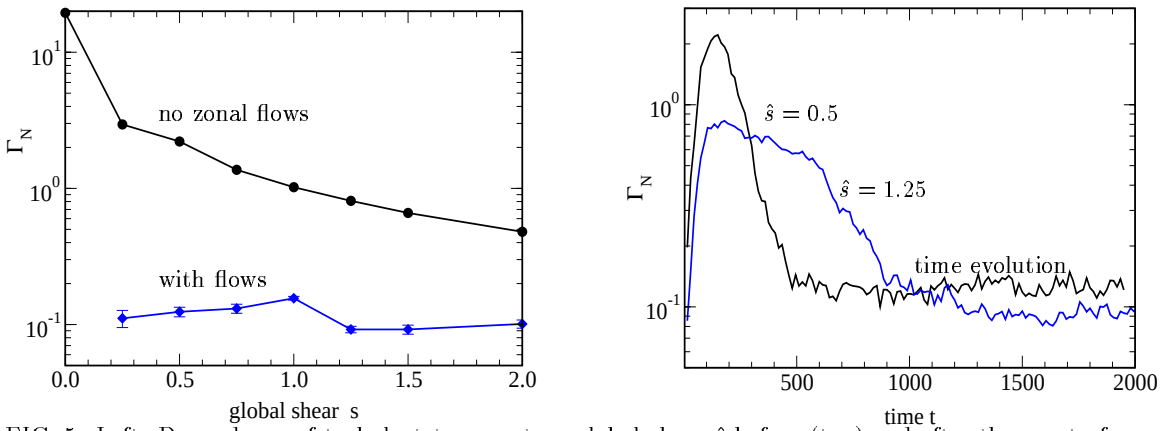

FIG. 5. Left: Dependence of turbulent transport on global shear $\hat{s}$ before (top) and after the onset of zonal flows. Right: time line of the simulation (with full dynamics) for $\hat{s} = 0.5$ (black) and $\hat{s} = 1.25$ (blue).

Zonal $E \times B$ flows are generated via Reynold stress by coupling of eddies to flows with both $k_y = 0$ and $k_{||} = 0$. By decorrelation of vortices and transfer of energy from eddies to the flow the turbulence amplitude is effectively lowered. For tokamak geometry the suppression effects have been shown to be a relevant part of the overall dynamics. Zonal flows are switched off in the computations by setting the flux surface average Reynolds stress $v_E \cdot \nabla\nabla^2\Phi$ to zero. In this case, the transport level is higher by a factor 2-5 in toroidal geometry compared to the case with full dynamics. For stellarator geometry, damping effects are also demonstrated over a range of various levels of collisionality $\hat{\nu}$. These results are shown in Fig. 6 (left) for $\xi = \zeta - q\theta = 0$.

Linear drift wave theory in Helias geometry suggests, that the parallel structure of the mode is governed by a combination of helical and toroidal ballooning. In our nonlinear turbulent simulations, however, no helical ballooning is observed. The drift wave structure limits itself to long parallel wavelengths, which average over the magnetic structure. We note especially a lack of asymmetry along the field line when the normal curvature departs from the simple sinusoidal form of a tokamak. Fig. 6 (right) shows minor variations in the turbulence amplitude along the field line, following more from the local shear than the normal curvature.

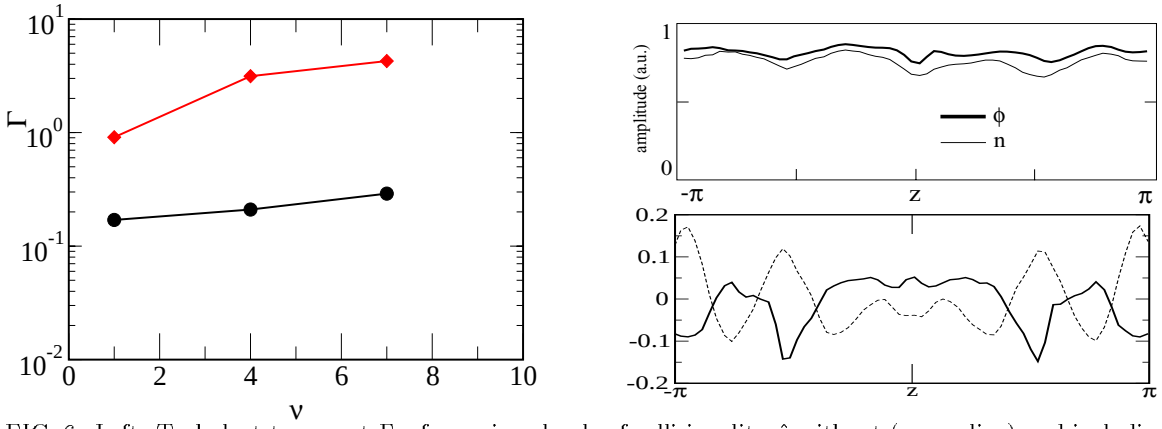

FIG. 6. Left: Turbulent transport Γ_N for various levels of collisionality $\hat{\nu}$ without (upper line) and including (below) zonal flows. Right: Mode structure (top) compared to $|B|$ (dotted line) and κ_N (solid line).

III. ACKNOWLEDGEMENTS

We thank S. Pinches, E. Strumberger and J. Kisslinger for providing the numerical equilibria, and F. Jenko for useful discussions and benchmark efforts. The experimental data have been obtained by H. Meister and the ASDEX Upgrade Team.

---

[1] A. Kendl, submitted to *Plasma Phys. Control. Fusion* (2001).
[2] H. Meister, A. Kallenbach, A. Peeters, A. Kendl, J. Hobirk and ASDEX Upgrade Team, accepted by *Nucl. Fusion* (2001).
[3] E. Strumberger, H. Wobig, J. Kisslinger and C. Nührenberg, *Proc. 26th European Conf. on Contr. Fusion and Plasma Physics*, Maastricht (1999)
[4] F. Jenko, W. Dorland, M. Kotschenreuther and B. Rogers, *Phys. Plasmas* **7**, 1904 (2000)
[5] B.D. Scott, Plasma Phys. Control. Fusion **39**, 1635 (1997).
[6] A. Kendl, B.D. Scott and H. Wobig, *Plasma Phys. Control. Fusion* **42** L23 (2000).